Evaluation of Crack Depth Using Eddy Current Techniques with GMR-based Probes

Ruben Menezes, Artur L. Ribeiro, Helena G. Ramos
Instituto de Telecomunicações, Instituto Superior Técnico
Universidade de Lisboa, Av. Rovisco Pais
1049-001 Lisboa, Portugal
hgramos@ist.utl.pt

***Abstract*— This paper presents experimental and simulated results obtained using the eddy current nondestructive method to conclude about the depth of linear cracks machined on an aluminum plate. Experimental tests were performed with a sinusoidal excitation field of fixed-amplitude and with a giant magnetoresistance-based sensor to measure the resultant magnetic field on the plate surface. To validate and better insight the experimental results, numerical simulations have been carried out with a commercial program for conditions similar to the experimental case studies. A scheme to infer about crack depth is proposed.**

Keywords—eddy current testing; crack sizing; crack depth; giant magnetoresistance sensor; GMR.

I. INTRODUCTION

Non-destructive evaluation (NDE) represents an important role in aerospace industry for an accurate evaluation of diverse types of flaws, such as fatigue cracks in aircraft metallic structures, without impairing its future usefulness. Nowadays, for the assessment of the expected life of mechanical components NDE is performed using different methods. Some non-destructive tests worth mentioning are: X-ray; ultrasonic testing and eddy-current testing [1,2].

The most critical defects associated with material fatigue and stress corrosion are crack like defects. For those defects, length and depth are typically much larger than their width. Therefore, to characterize the defects, the main parameters of interest are the length and the depth profile. For the crack length the location of the magnetic field peaks proved to give a good estimate [3]

Eddy-current inspection is fast and effective in detecting defects such as fatigue cracks, inclusions, voids and corrosion that occur in conductive materials [4,5]. The application of time-variable magnetic fields induces eddy currents in the conductive specimens. The presence of defects acts as high resistance barriers. This disturbs eddy current paths and this disturbance is manifested in the magnetic flux density that can be measured using different kinds of probes. An excitation coil with air or ferrite core sensing coils are examples of probes solution used in the industry to detect surface defects [6,7]. However, to increase the capability of defect detection, other solutions have been developed using an excitation coil with magnetic sensors such as Hall [8], SQUIDS [9] or magneto-resistance based [10] sensors (anisotropic or giant).

This work presents an automatic measurement system that includes a giant magnetoresistance (GMR) based eddy-current probe to detect and characterize depth profile of straight defects artificially machined in an aluminum plate. The directional characteristics, high sensitivity and frequency response (10 Hz to 1 MHz) provided by the GMRs makes them good candidates in the application of defect detection. By measuring the magnetic field amplitude and phase originated from the induced eddy currents in the plate it is possible to obtain information about the defect location and its geometrical characteristics [11]. Low frequency excitation is used increasing the standard depth penetration of the fields in the material. Crack depth can be estimated by interpreting the obtained field perturbation [12]. The measured values depend on the conductivity of materials, magnetic permeability, excitation frequency, current intensity, lift-off effect (distance between probe and specimen) [13] and discontinuities or non-homogeneities in material. In order to interpret the experimental data, a finite element model (FEM) has also been used to preview the measurements for a given excitation and crack geometry. A comparison between experimental and simulated data is carried out and conclusions are drawn.

II. SYSTEM DESCRIPTION

A. GMR-based eddy-current probe

The excitation coil of the eddy current probe (ECP) is a pancake-type with a GMR sensor embedded on the lower level and presenting the active plane perpendicular to the coil axis. The sensor is located with its sensitive axis parallel to the plate under inspection. Thus the excitation field on the coil axis, being perpendicular to the sensing axis of the GMR, is not sensed. The induced eddy currents have circular symmetry in case of a defect free aluminum plate, which will produce no effect on the GMR sensor output. From the various GMR sensors produced by Non Volatile Electronics (NVE) the AA002-02 was the elected for this work because it presents a high sensitivity [3.0; 4.2] mV/V-Oe [14]. In order to study depth profiles defects the sensor output voltage is processed. The probe geometry is shown in Fig. 1 and the dimensions of the used coil in the defect detection experiment are given in Table 1. In order to put the sensor working in its linear range, biasing is carried out with a permanent magnet. A holder with the coil, the sensor and some signal conditioning circuitry was designed to reach a more stable position with a constant lift-

978-1-4799-7569-3/15/$31.00 ©2015 IEEE

off during the automatic scan, which represents one of the most significant errors that affects the measured data.

TABLE 1 Parameters of the ECP excitation coil.

Excitation Coil Parameters	
Inner diameter	10 mm
External diameter	20 mm
Length	9.5 mm
Round wire diameter	0.56 mm
Number of turns	115
Lift-off	0.5 mm
Conductivity	60 MS/m
Excitation current	0.2 A

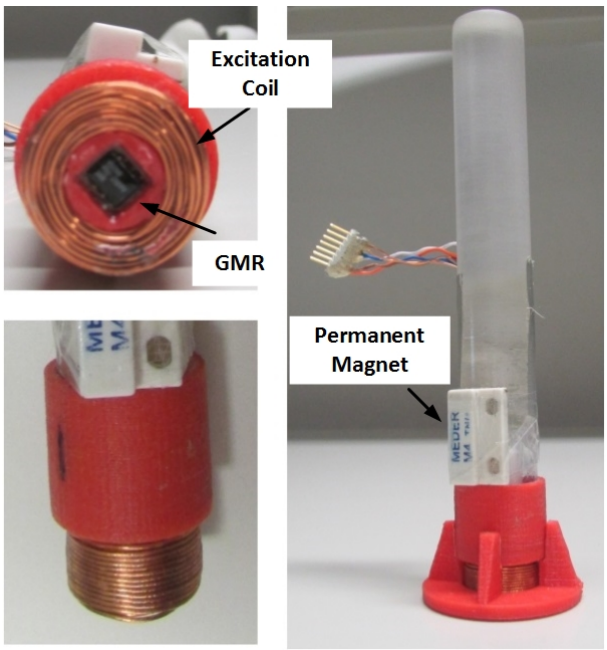

Fig. 1. Photographs of the eddy-current probe used in this work.

B. Automatic Measuring System

Measurements are carried out using a XY-automated positioning system to scan the material under test, controlled by a RS232 interface inserted in a PXI-1036 chassis from National Instruments. The scanned area can be (40x35) cm2 and the permissible speed of each single axis module is 810 mm/s, with minimum steps of 0.05 mm. The signal sensed by the GMR, at each probe position, is acquired using a multifunction Data Acquisition (DAQ) board NI PXI-6251 inserted in the PXI chassis and remotely controlled by a PC [15]. This board is composed by sixteen 16-bit sampled analog input channels and 7 input ranges from ±0.1 V to ±10 V with maximum sampling rate 1.25 MS/s per channel. AC current is imposed to the coil with fixed amplitude and frequency through a FLUXE 5700A calibrator controlled by GPIB interface and is constantly monitored by the DAQ board using a 10 Ω sensing resistor (RS). The magnetic sensor is powered by a Calex BPS4000 with ±12 V. The entire scanning is driven and monitored running a MATLAB® program on a PC. The used architecture system is depicted in the Fig. 2.

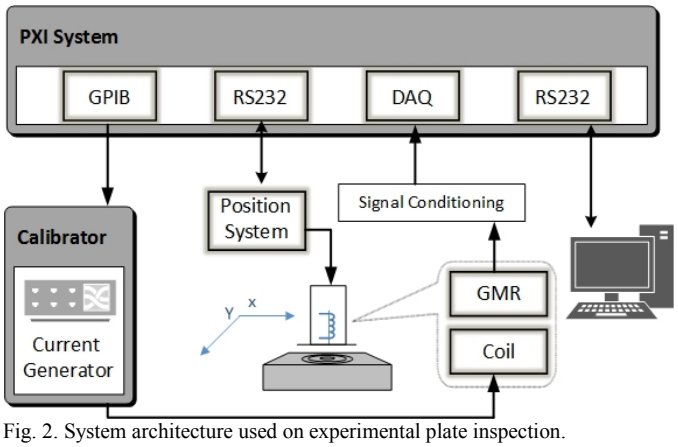

Fig. 2. System architecture used on experimental plate inspection.

C. Discription of the samples

The specimen under test is a plate of thickness 4 mm, made of an aluminum alloy (1050) with a conductivity σ = 35.6 MS/m. On this plate there are 21 different linear and superficial defects with the same width (1 mm). The cracks have 7 different values of depth (from 0.5 mm to 3.5 mm with 0.5 mm steps) and for each one there are 3 lengths (5 mm, 8 mm and 12 mm). The plate is 40 cm in one direction and 35 cm on the orthogonal one.

D. Conditions of Experiments

Experiments are carried out scanning an area around each defect with the probe. The positioning system moves the probe over the sample with 1 mm of resolution. The amplitude of the GMR output voltage is stored and associated with its corresponding position. The excitation current is 0.2 A and the operating frequency 250 Hz. Low frequency ensures total plate penetration along crack depth axis, which skin depth of penetration is δ=5.4 mm, in the sample under test.

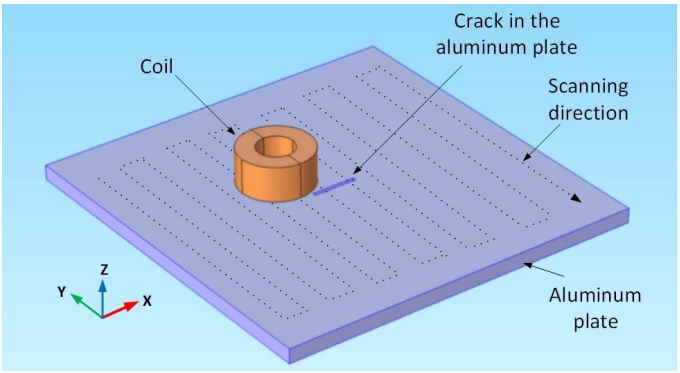

Fig. 3. View of a 3-D model multi-turn coil and its path over an aluminum plate with a defect.

Two scans are carried out as depicted in Fig. 3: one with the GMR sensing axis aligned with the longitudinal axis of the defect and the other in the orthogonal direction. The probe is rotated 90º to shift the scanning direction and the magnetic components, B_x and B_y are measured, respectively.

III. Finite Element Model

A simulation model validates the experimental results. The model, depicted in fig. 4, is created with the same experimental characteristics and for the same conditions as the experimental case studies. The simulations were performed using a Finite Element Method software, COMSOL® Multiphysics.

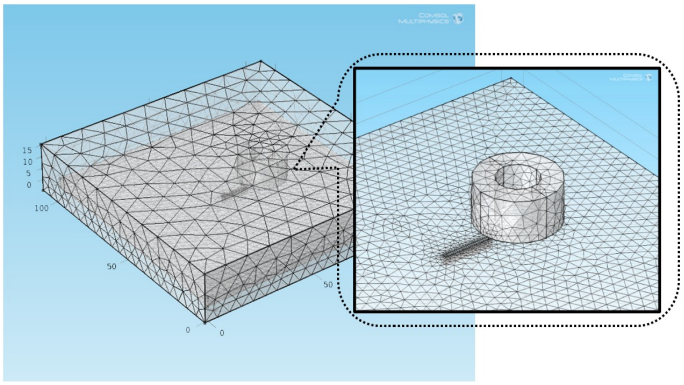

Fig. 4. Mesh appearance on the simulated model.

Because meshing an infinite volume cannot be afforded, it is necessary to specify a volume to mesh and solve for. In this case it make sense to enclose the coil and the plate in a block, in a concentric way. To get accurate results, the mesh in the aluminum plate is finer than in the rest of the geometry. For the same reason the grid is also finer in the vicinity of the defect, which is the area of interest.

IV. Results

To estimate the depth of open cracks the perturbations of both components of the magnetic field are analyzed and features extracted from data determined experimentally and with a numerical model.

Experiments were performed with the setup described in Section II, scanning an area over the crack. Liftoff was determined to be 1 mm. Acquisitions were done with an excitation current of 0.2 A and frequency 250 Hz. Data was digitally processed and the value corresponding to a constant plane of complex value was subtracted from data results. Fig. 5 and 6 show data measured and data determined using the numerical model for similar conditions. In order to speed up the numerical simulation procedure in both simulations the area over the crack is less that the area that was experimentally scanned. Fig. 5 depicts the magnetic flux density in the direction of the crack and Fig. 6 in the perpendicular direction.

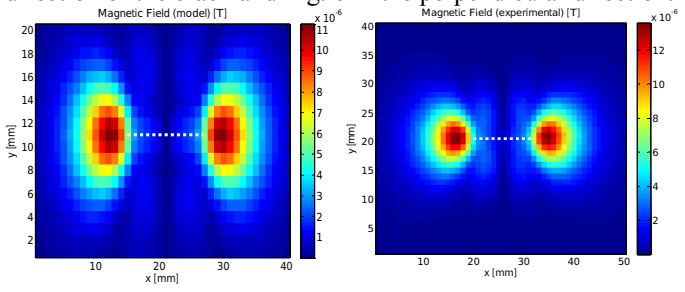

Fig. 5. Scanning map showing the disturbed magnetic field component parallel to the crack lines (B_x). Comparison between simulation model and experimental scanning for a 12 mm long and 3 mm deep defect.

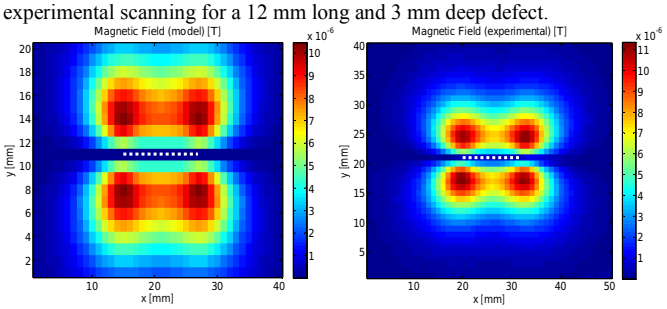

Fig. 6. Scanning map showing the disturbed magnetic field component orthogonal to the crack lines (B_y). Comparison between simulation model and experimental scanning for a 12 mm long and 3 mm deep defect.

Experimental and simulated results agree satisfactorily. Differences are justified by the misplacement of the GMR sensor in the center position of the bottom of the probe (eventually presenting some tilt), liftoff uncertainty and also due to the fact that in the model the magnetic flux is calculated for a specific position and experimentally the magnetic flux density is assessed by a sensor with physical dimensions. Nevertheless one may conclude that when the GMR sensor is aligned with the crack longitudinal axes, B_x, two magnetic field peaks located on both crack tips are observed. On the orthogonal direction B_y presents four peaks.

Fig. 7 presents the results for B_y obtained experimentally and with the model for three different values of the 12 mm crack depth (d = 1, 2 and 3 mm) when an area around a crack is scanned.

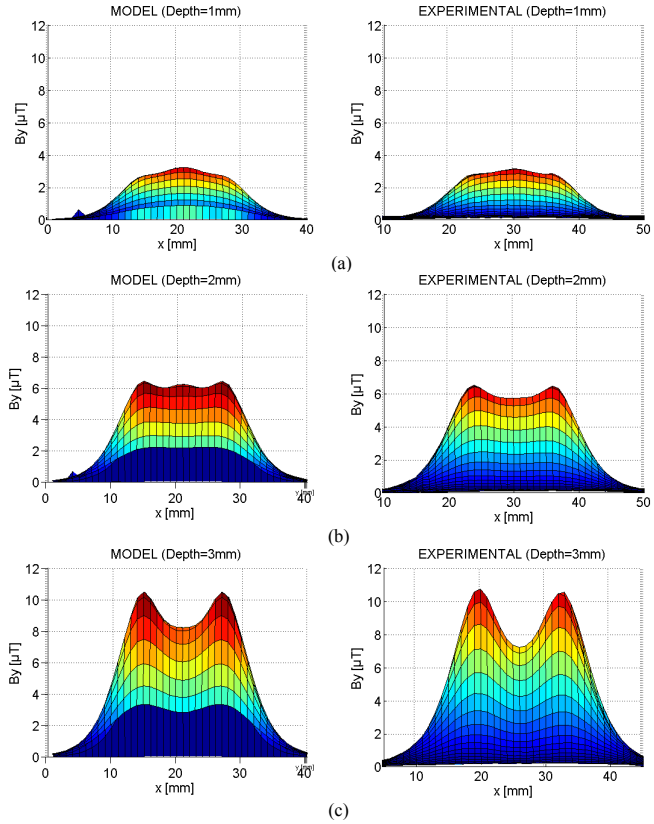

Fig. 7. Magnetic flux density amplitude, B_y component: (a) depth = 1 mm; (b) depth = 2 mm; (c) depth = 3 mm.

When an area around a crack is scanned the profile of both components of the magnetic field along the crack are obtained experimentally in amplitude and phase. In order to study the depth of an open crack it was observed that the best feature is the amplitude value of the magnetic field component. Small disturbances are observed in the phase of the magnetic field component. Results obtained for B_x for the same different crack depths are depicted in Figs. 8 (a) (b) and (c).

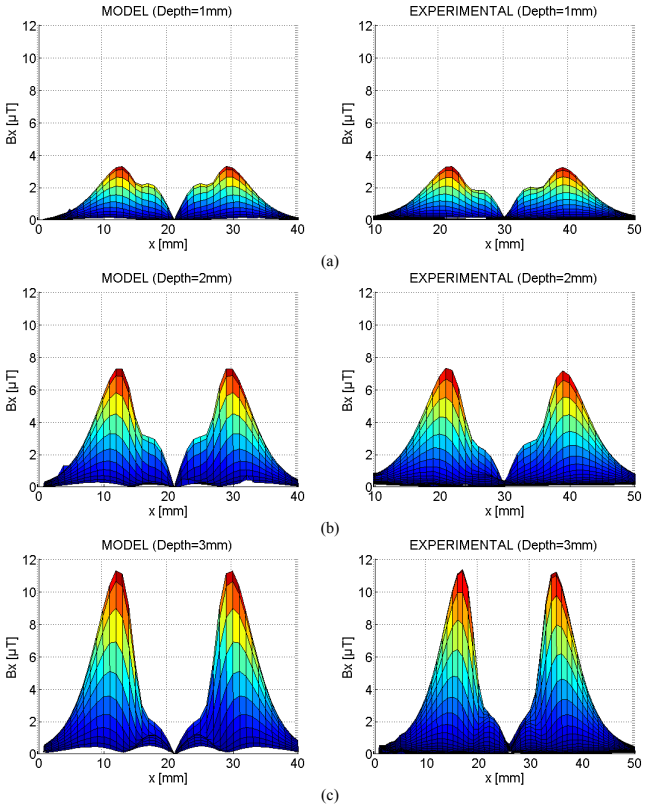

Fig. 8. Magnetic flux density amplitude, B_x component: (a) depth = 1 mm; (b) depth = 2 mm; (c) depth = 3 mm.

Figs. 7 and 8 show that the amplitude of the magnetic field density for both components, increases with increasing superficial crack depth. This effect is expected because with deeper defect, with larger volumes, a higher density of eddy currents is affected and higher perturbations on the secondary field are observed. This is also evidenced by the simulation model. Fig. 7 stresses also that when the depth of the defect increases, the maximum values of the field move from to middle line along the crack length to the crack tips vicinity.

According to the presented results, it is clear that the magnetic flux density is closely correlated with the crack's depths and a relation may be established between the peaks observed in the amplitude profiles of the magnetic field density and crack depths. This fact could be used to establish the method for the determination of the depths. For B_y the best profile to establish this relation must be taken along a line longitudinal to the crack and containing the two peaks and conclusions are not evident. For B_x it is a much more defined profile because only two peaks appear when the region over the crack is scanned and they are always positioned along the longitudinal lines of the crack and close to the crack tips. Fig. 9 show the magnetic flux density component peaks amplitude and the corresponding crack depth when a 12 cm length crack is scanned over. Fig. 9 (a) depicts a linear behavior between the magnetic flux density amplitude peaks of B_x and the crack depth. This behavior is accurate up to 3 mm depth. This behaviour can be generalized to other depths but accuracy decreases with defect length.

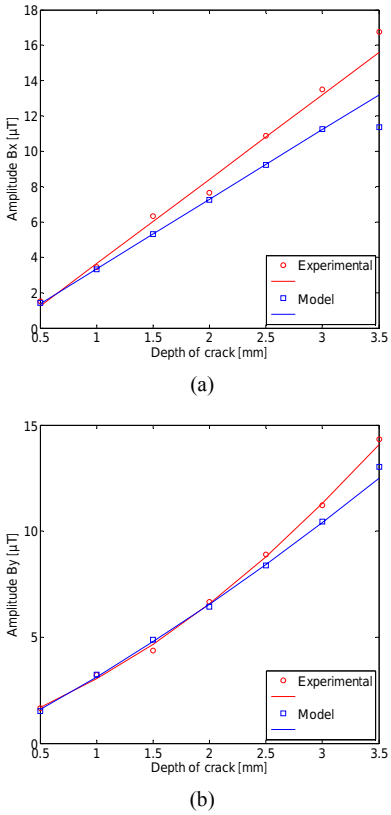

Fig. 9. Amplitude peak of magnetic flux density for seven different crack depths when the magnetic field is: (a) parallel or (b) perpendicular to the crack length.

These results show clearly the main drawback of using eddy current methods to evaluate crack depths in metallic surfaces. In principle, it is possible to estimate crack depth by comparing the eddy current signal from an unknown crack against data from a calibration of a similar crack length in the same material. In practice this is not exact due to the influence of the crack depth and the aspect ratio (ratio of length to depth) on the estimation of crack depth. Results were taken for a frequency equal to 250 Hz, corresponding to a standard penetration depth, $\delta = 5.4$ mm. Nevertheless, the aspect ratio determines now the eddy currents overcome the barrier imposed by the defect presence, changing its circular path either going around the crack or passing under it [16, 17].

From the results obtained for magnetic field disturbance a variation is detectable in energy with the change of the crack's depth. It was decided to perform a case study, containing open cracks with several depths and lengths, in order to characterize the behavior of the magnetic field energy. The results are shown in Fig. 10 with normalized values for the energy.

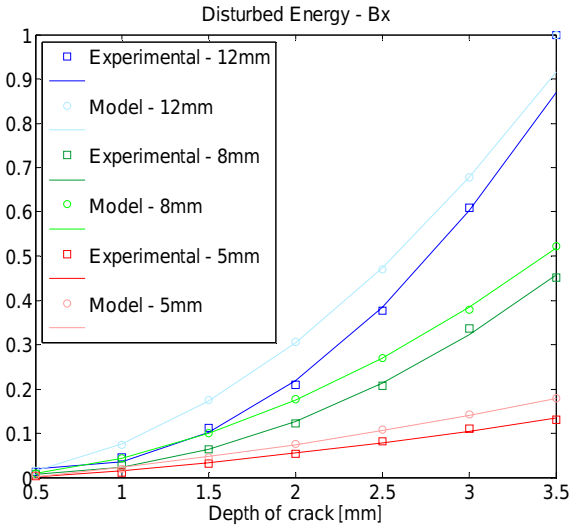

(a)

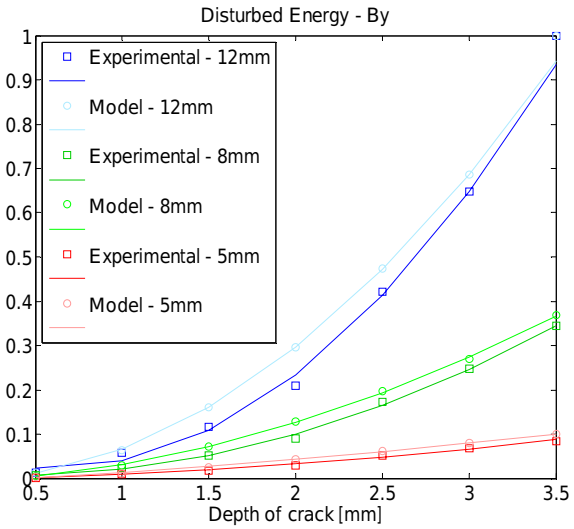

(b)

Fig. 13. Energy variation with the depth for 3 different length values, normalized relatively to the maximum observed value.

V. Discussion and Conclusion

In this paper the magnetic field density is determined experimentally and with a numerical method when an aluminum sample plate with different machined crack depths is scanned. All experimental results are corroborated by the simulated model, throughout a large amount of case tests.

The results presented show a clear magnetic flux density amplitude maximum disturbance that depends on the crack depth. It is demonstrated that for cracks with a depth much less the standard penetration depth (δ) for the excitation frequancy, the method can be applied to evaluate the crack depth. However, it is also true, that the method depends on the aspect ratio (ratio of length to depth) on the estimation of crack depth. It is observed that for low depths, compared to defect length, currents pass underneath de flaw, whereas in presence of a deeper defect, the shortest path for these same currents is go around the crack.

Acknowledgment

This work was developed under the Instituto de Telecomunicações project EvalTubes and supported in part by the Portuguese Science and Technology Foundation (FCT) projects: UID/EEA/50008/2013, SFRH/BD/81856/2011 and SFRH/BD/81857/2011. This support is gratefully acknowledged.

References

[1] B. P. C. Rao, Practical Eddy Current Testing, Alpha Science International Ltd., 2007, pp.1-17

[2] P. E. Mix, Introduction to Nondestructive Testing: A Training Guide, 2nd ed., Wiley-Interscience, May 2005

[3] A. Bernieri, L. Ferrigno, M. Laracca and M. Molinara, "Crack Shape Reconstruction in Eddy Current Testing Using Machine Learning Systems for Regression", IEEE Trans. Instrum. Meas., vol. 57, no. 9, pp. 1958-1968, September 2008.

[4] D. Pasadas, T. Rocha, H. Ramos and A. Ribeiro, "Evaluation of portable ECT instruments with positioning capability", Measurement, vol. 45, no. 3, pp. 393-404, 2012.

[5] J. R. Bowler and N. Harfield, "Evaluation of probe impedance due to thinskin eddy current interaction with surface cracks", IEEE Trans. Magnetics, vol. 34, no. 2, pp. 515-523, March 1998.

[6] A. Bernieri, G. Betta and L. Ferrigno, "Characterization of an eddy-current-based system for nondestructive testing", IEEE Trans. Instrum. Meas., vol. 51, no. 2, pp. 241-245, April 2002.

[7] A. Ribeiro and H. Ramos, "Inductive probe for flaw detection in non-magnetic metallic plates using eddy-currents", Proc. IEEE Instrumentation and Measurement Technology Conf, Victoria, Canada, pp. 1447-1451, May 2008.

[8] Y. He, F. Luo, M. Pan, F. Weng, X. Hu, J. Gao and B. Liu, "Pulsed Eddy Current Technique for Defect Detection in Aircraft Riveted Structures", NDT & E International, vol. 43, no. 2, pp. 176-181, March 2010.

[9] C. Carr, D. Graham, J. C. Macfarlance and G. B. Donaldson, "HTS SQUIDs for the non-destructive evaluation of composite structures", Inst. Of Physics, Supercond. Sci. Technol, no. 16, pp. 1387-1390, 2003.

[10] A. Jander, C. Smith and R. Schneider, "Magnetoresistive sensors for nondestructive evaluation", Proceedings – SPIE, The Internat. Society For Optical Engineering 5570, 2005, pp. 1-13.

[11] N. Nair, V. Melapudi, H. Jimenez, X. Liu, Y. Deng, Z. Zeng, L. Udpa, T. Moran, S. Udpa, "A GMR-based eddy current system for NDE of aircraft structures", IEEE Trans. Maagnetics, vol. 42, no. 10, pp. 3312-3314, October 2006.

[12] D. J. Pasadas, A. Lopes Ribeiro, T. J. Rocha and H. Geirinhas Ramos, "Open crack depth evaluation using eddy current methods and GMR detection", Proc. IEEE Metrology for Aerospace Conf., Benevento, Italy, pp. 117-121, May 2014.

[13] A. Bassam, A. Abu-Nabah, P. B. Nagy, "Lift-off effect in high-frequency eddy current conductivity spectroscopy", Elsevier Independent Nondestructive Testing and Evaluation, vol. 40, no. 8, pp. 555-565, December 2007.

[14] NVE Magnetic Sensor Catalog, www.nve.com/sensorcatalog.php.

[15] National Instruments site, www.ni.com/products/.

[16] H. G. Ramos, T. Rocha, A. L. Ribeiro, and D. Pasadas, "Determination of Linear Defect Depths from Eddy Currents Disturbances", Proc. Review of Progress in Quantitative Nondestructive Evaluation – QNDE, Baltinore, United States, July 2013.

[17] M. Raja, S. Mahadevan, B. Rao, S. Behera, T Jayakumar, "Influence of crack length on crack depth measurement by an alternating current potential drop technique", Measurement Science and Technology, 21 (2010) 105702, IOP Publishing.